AIR FORCE REPORT NO.
SAMSO-TR-69-55

AEROSPACE REPORT NO.
TR-0200(9990)-1

Influence of Concentrated Lateral Loads on the Elastic Stability of Cylinders in Bending

Prepared by S. OKUBO
Aerodynamics and Propulsion Research Laboratory
P. E. WILSON
Applied Mechanics Division
J. S. WHITTIER
Aerodynamics and Propulsion Research Laboratory

68 DEC 15

Laboratory Operations
AEROSPACE CORPORATION

Prepared for SPACE AND MISSILE SYSTEMS ORGANIZATION
AIR FORCE SYSTEMS COMMAND
LOS ANGELES AIR FORCE STATION
Los Angeles, California

Air Force Report No.
SAMSO-TR-69-55

Aerospace Report No.
TR-0200(9990)-1

INFLUENCE OF CONCENTRATED LATERAL LOADS ON THE ELASTIC STABILITY OF CYLINDERS IN BENDING

Prepared by

S. Okubo
Aerodynamics and Propulsion Research Laboratory

P.E. Wilson
Applied Mechanics Division

J.S. Whittier
Aerodynamics and Propulsion Research Laboratory

68 DEC 15

Laboratory Operations
AEROSPACE CORPORATION

Prepared for

SPACE AND MISSILE SYSTEMS ORGANIZATION
AIR FORCE SYSTEMS COMMAND
LOS ANGELES AIR FORCE STATION
Los Angeles, California

FOREWORD

This report is published by the Aerospace Corporation, El Segundo, California under Air Force Contract No. F04701-68-C-0200. The report was prepared by S. Okubo of the Aerodynamics and Propulsion Research Laboratory, P.E. Wilson of the Applied Mechanics Division, and J.S. Whittier of the Aerodynamics and Propulsion Research Laboratory, in order to document research carried out from July 1967 to May 1968 under the above contract.

This report was submitted to George J. Babin, SMTTM, USAF, for review and approval on 29 January 1969.

The authors are indebted to M. L. Lundquist and Lt. G. Babin for assistance with the experiments and to Mrs. J. Lesser for data reduction calculations.

Approved

W.F. Radcliffe, Director,
Engineering Analysis Subdivision
Applied Mechanics Division

G.W. King
Vice President and General Manager
Laboratory Operations

Publication of this report does not constitute Air Force approval of the report's findings or conclusions. It is published only for the exchange and stimulation of ideas.

George J. Babin, 1st Lt., USAF
Project Officer

ABSTRACT

The character of the instability and the degradation of the moment-carrying capacity are found by Mylar model experiments for cylinders in bending when subjected to concentrated lateral loads. Lateral loads can seriously degrade the moment capability of cylinders. Critical combinations of moment and lateral load cause two distinct modes of failure - collapse and snapping. Collapse modes exhibit buckles which cover the compression half of the cylinder and are critical for large values of moment and small values of lateral load. Snapping modes of failure involve a single dimple and exist for smaller values of moment and larger values of lateral load.

CONTENTS

FIGURES

SYMBOLS

D	=	bending rigidity, see Eq. (4)
E	=	Young's modulus
L	=	length of shell
M	=	bending moment
P	=	axial force
P^*	=	particular value of axial force, see Eq. (1)
p	=	internal pressure
Q	=	magnitude of a lateral load
R	=	radius of shell
S_i	=	designation for spatial distribution of loads, see Fig. 1
t	=	thickness of shell wall
ν	=	Poisson's ratio
δ	=	radial displacement
σ	=	axial stress

SECTION I

INTRODUCTION

This paper is concerned with elastic stability of circular cylindrical thin shells in bending. Of special interest are instabilities manifested when one or more concentrated loads act normal to the wall of such a shell. A description of the load combinations studied is aided by Fig. 1. As shown in this figure, from one to nine lateral loads, each of magnitude Q, are applied in spatial distributions designated S_1 through S_6. Also acting are bending moment M, axial force P, and internal pressure p. In the present work, the axial force P is restricted to that value P^* needed to equilibrate the internal pressure on the end wall, i.e.

$$P = P^* \equiv \pi R^2 p \qquad (1)$$

where R is the shell radius. The objective of this study is to determine for each lateral loading S_i the combination of loads (M, Q, p, P^*) for instability and the character of the instability.

To the authors' knowledge, no previous work has been primarily directed to this problem. For limiting cases with no lateral loads (M, 0, p, P) there is extensive literature. Work by Weingarten,[1] and also by Weingarten, Morgan, and Seide[2] is especially pertinent. The influence of a concentrated lateral load on the stability of an unpressurized cylinder under axial compression has been studied experimentally by Ricardo[3] and Babcock.[4] In the notation of Fig. 1, their studies were concerned with spatial distribution S_1 and loads (0, Q, 0, P).

The present investigation was carried out by nondestructive model experiments employing shells of Mylar. Loading was accomplished with dead weight fixtures. A majority of the experiments used shells with

SPATAL DISTRIBUTION	Q AXIAL SPACING
S_1 , S_4	L/2
S_2 , S_5	L/3
S_3 , S_6	L/4

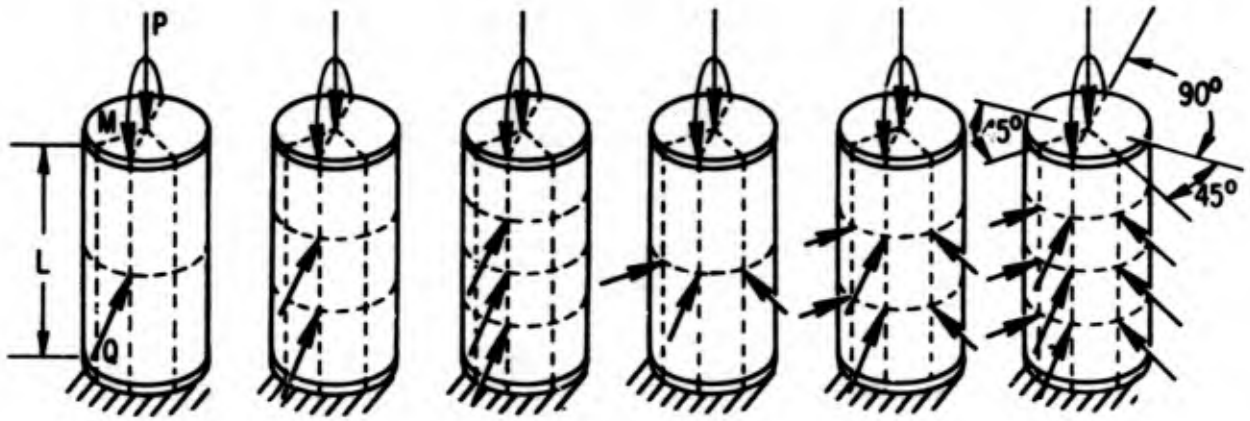

S_1 S_2 S_3 S_4 S_5 S_6

ALL LATERAL LOADS HAVE MAGNITUDE Q

Fig. 1. Loads Considered

geometric parameters $L/R = 2.33$ and $R/t = 371$, and internal pressure parameter $(p/E)(R/t)^2 = 0$ and 0.09. Critical combinations of M and Q were found for spatial distributions S_1 through S_6. Five shells were tested to form an estimate of the experimental scatter. Because of the large number of tests already involved, it was beyond the scope of the present program to carry out any extensive study of the effect of different shell geometries. However, a shell with $L/R = 1.0$ was tested for spatial pattern S_1.

Results of the experiments indicate that small lateral loads can significantly degrade the moment capability of cylinders by precipitating two types of instability - collapse and snapping. Collapse modes exhibit diamond-shaped buckles which cover the compression portion of the cylinder, whereas snapping modes involve one or more localized dimples at the lateral load application points. The effect of a small lateral internal pressure is to cause a substantial strengthening without changing the character of the failure modes. Influences of length-radius ratio and sequence of load application are examined, and for the parameters investigated, are found to be of minor importance. Data repeatability for identical load cycles on a specific model is excellent. Results are presented for five shells to give an indication of the experimental scatter. Following a suggestion by Seide,[5] pertinent buckling load interaction data are normalized in such a way as to infer greater generality.

SECTION II

EXPERIMENTS

A. SHELL MODELS

Cylindrical shell models for nondestructive buckling tests were fabricated from Type A Mylar. The large elastic strains possible with this material permit repeated buckling (with limited deflections) without injury to a model. All cylinders were made from the same roll of Mylar. The Mylar thickness was 0.014 ± 0.0005 in., and its modulus of elasticity was determined to be 625,000 psi in compression and 595,000 psi in tension.

A model was formed by rolling the sheet stock over a circular mandrel and joining the ends at a longitudinal seam butt-joint. At the joint, 1-in.-wide overlays of 0.014-in. Mylar were bonded to the inner and outer surfaces of the shell for reinforcement. The reinforced butt-joint was used in preference to a lap-joint to obtain a more nearly circular shell. To minimize the influence of the joint, all tests were conducted with the seam located at the plane of zero bending stress. Clamped end conditions were approximated by bonding the ends of the shell model in deep grooves provided in heavy aluminum rings. The models had a nominal inside diameter of 10.40 in. and a length of 12.10 in.

Deviations from circularity were measured to assess the degree of imperfection of the models. Readings of radial deviations from a mean circular shape were taken at transverse planes located 3, 6, 9, and 11 in. from the lower end of a model. Data for Cylinder 4 are shown in Fig. 2. These data are typical in that the radial deviations except at the seam (located at 0-deg) do not exceed 0.013 in. (nearly one wall thickness).

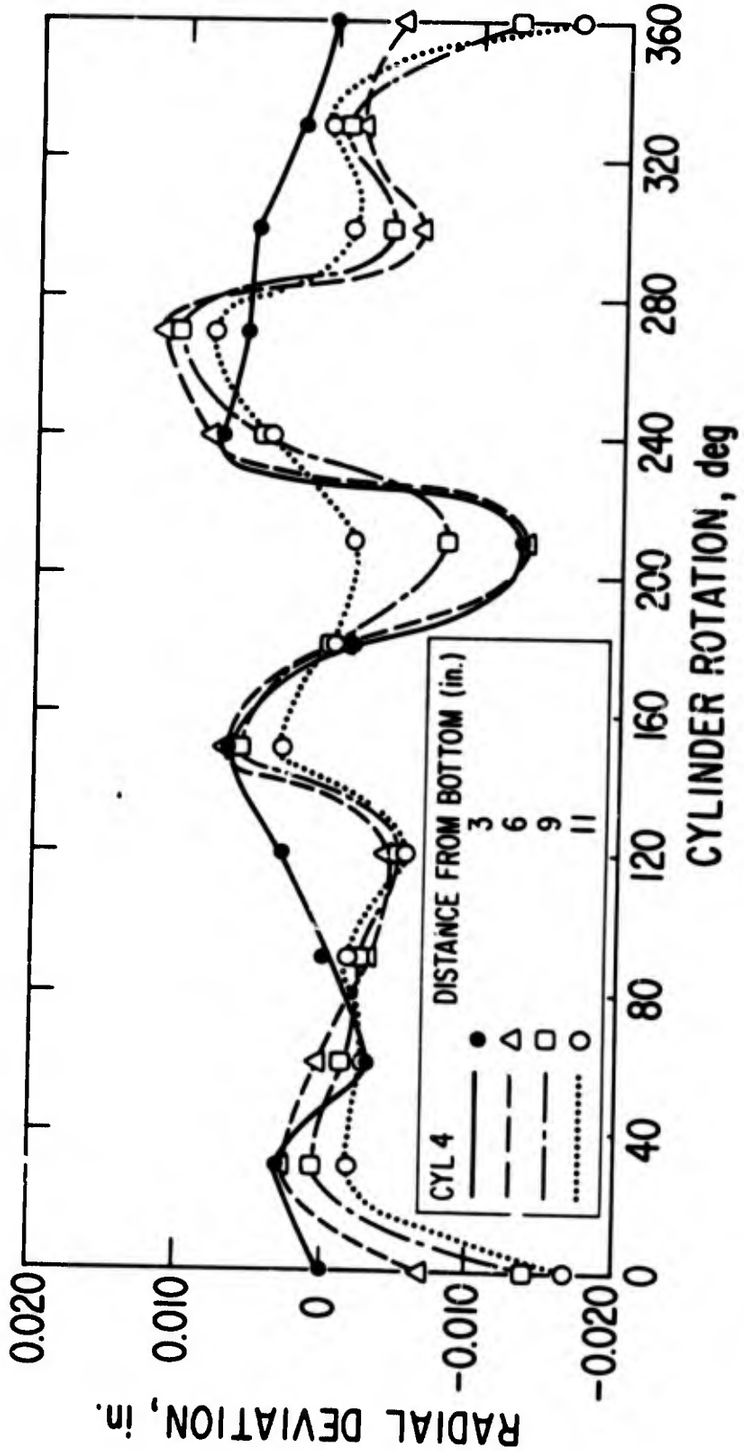

Fig. 2. Deviations from Circularity

The single exception to this generalization was Cylinder 5 for which a 0.020-in. deviation was observed. As might be expected, Cylinder 5 performed poorly under load relative to the other models.

Five test cylinders were fabricated. During the tests, Cylinder 2 was found to be defective and was discarded to salvage the end rings. Hence, data for Cylinder 2 are not presented.

B. TEST APPARATUS

The apparatus for applying a bending moment and concentrated radial loads to a shell model is shown in Fig. 3. The moment-producing forces are applied to the ends of the horizontal bar atop the cylinder by a cord and pulley system with dead weight loads. The loading system was calibrated by measuring with a load cell the net force exerted at each end of the moment bar as a function of the applied dead weight load.

An assembly of nine bell-crank levers utilizing dead weight loads was used to apply concentrated radial forces to the shell wall. This assembly is on the left side of the shell model in Fig. 3. The minimum radial load increment employed in the tests was 0.002 lb. Compared to this load increment pivot friction had a negligible effect (a change in pan load of 0.00015 lb was sufficient to overcome friction and cause substantial displacement of a lever).

Radial displacements of the shell wall were measured using a linear variable differential transformer assembly mounted inside the model. The transformer core was supported as a bifilar pendulum. In this way, it was possible to arrange for the contact force with the shell wall to be only on the order of 0.0002 lb.

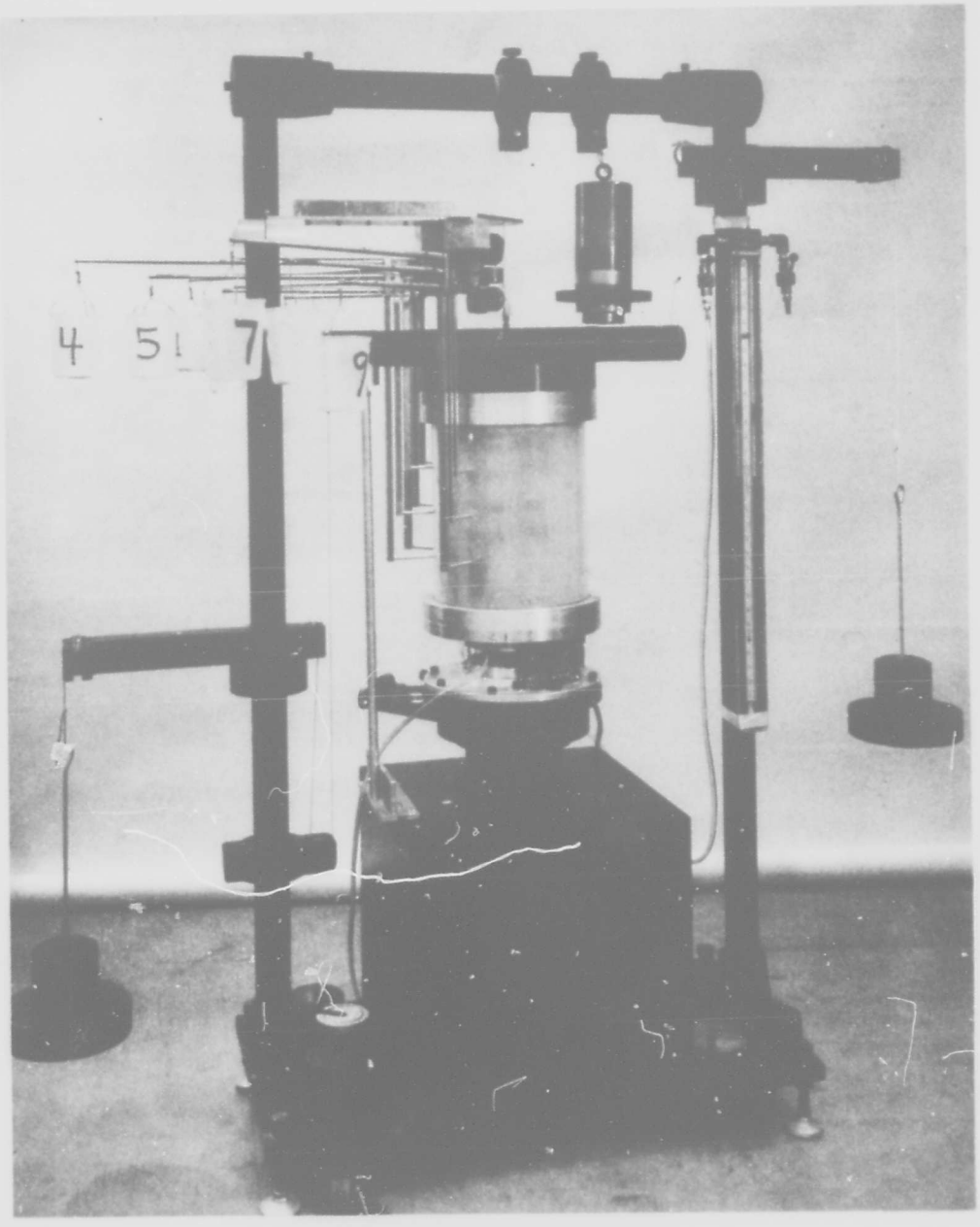

Fig. 3. Apparatus for Combined Flexural and Lateral Loading of Shell Models

The large metal counterweight assembly, above and to the right of the shell model in Fig. 3, was used to cancel all (or a portion of) the weight of the fixtures atop the model. Selection of the proper counterweight allowed application of the desired axial load. Internal pressurization of a cylinder was accomplished using nitrogen gas. An oil manometer (visible to the right of the shell model) was used to measure the pressure. The long slender rod to the left of the model is a mechanical stop to arrest the motion of the moment bar and thus limit the postbuckling deflections.

C. TEST PROCEDURE

For the determination of critical load combinations, the usual procedure was to apply the radial loads S_i and then increase the moment until buckling or snapping occurred. For each level of radial load, the critical moment determination was repeated a minimum of four times to obtain an average. Repeatability was good; the usual moment variation was less than 1 percent. A check on the possible effect of the sequence of loading showed that it was significant only in a special case to be discussed later. The test procedures for both the pressurized (0.4 psi) and unpressurized models were identical except that the previously mentioned counterweight was changed to maintain zero net axial load.

Shell wall deflections were measured at the cylinder midpoint on the meridian of maximum compressive bending stress for the case of S_1 loading. The tests showed that the prebuckling deflection for any (M, Q, p, P^*), relative to zero deflection for $(0, 0, p, P^*)$, was independent of the loading sequence.

SECTION III

EXPERIMENTAL RESULTS AND DISCUSSION

Of the six radial load patterns investigated (see Fig. 1), the simplest—i. e., pattern S_1—was investigated the most extensively. Subsequent tests with multiple radial loads revealed mainly that the results for S_1 typified the rest. For the multiple load combinations investigated, no new phenomena were obvious. For this reason our discussion deals mainly with case S_1.

The two types of failure observed in the tests are shown in the photographs of Fig. 4. These photographs show typical postfailure deflection patterns observed for the case of a single radial load* (spatial pattern S_1) for both unpressurized and pressurized models. Either type of failure is an example of structural instability in that an abrupt increase in deformation results from a very slight increase in load. Snapping failures, illustrated by Figs. 4a, 4b, are characterized by the postfailure appearance of a local dimple under the radial load. For pressurized models, smaller dimples were observed (e. g., Fig. 4b), even though the snapping loads were somewhat larger. Collapse failures, illustrated by Figs. 4c, 4d, are characterized by the postfailure appearance of an extensive diamond buckle pattern over the compression side of the shell. The buckle wavelength is significantly smaller for the pressurized model. In practice, postfailure collapse deformations would likely be much more severe than those shown in Fig. 4, since in these experiments the deformations were limited by a mechanical stop to avoid destruction of the models.

*The three levers visible on the right in each picture are not in contact with the model.

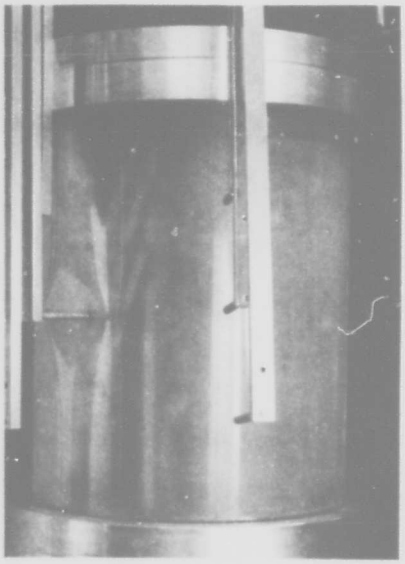

a. Snap, Unpressurized

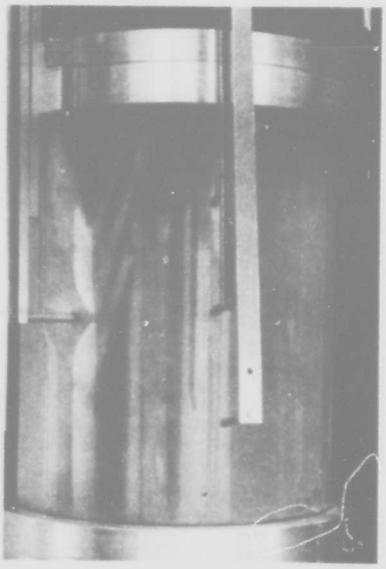

b. Snap, Pressurized

c. Collapse, Unpressurized

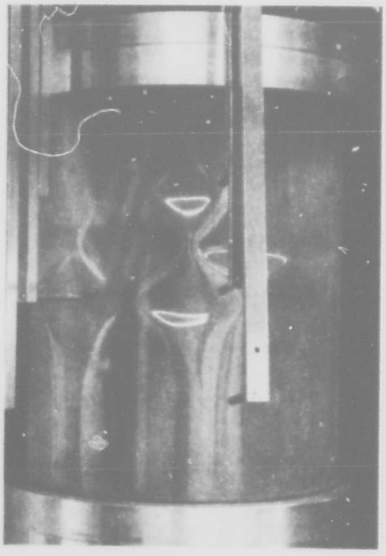

d. Collapse, Pressurized

Fig. 4. Typical Post-Failure Deformation Patterns

Shell wall deformation characteristics for a model subjected to various bending moments are illustrated in Fig. 5. This figure presents radial load vs. radial deflection (Q vs. δ) curves for Shell 4 with zero internal pressure for several values of bending moment. The radial load is applied in spatial pattern S_1, and the deflection is measured directly under the load. For this plot, deflections are reckoned with respect to the position of the shell wall with zero radial load, but after the moment is applied. The dashed portions of each curve represent unstable behavior where an abrupt increase in deflection occurs for a small increase in load. The lowest curves are for the largest values of bending moment. For large moments, the shell wall is softer with respect to radial loads in the stable range and the instability observed is collapse.

Snapping of the shell wall is observed for intermediate moments. Final postsnapping deflections are too large to plot to this scale and thus are noted on the curves. It was found that the postsnapped shells would sustain additional radial load and that a sufficient increase of radial load would cause collapse. Although one expects the load deflection curves to exhibit a horizontal tangent just before snapping, such behavior is not obvious in the curves of Fig. 5. Possibly further study directed to the shape of these curves and to the use of smaller load increments than those achieved with the present apparatus could resolve this point.

Snapping no longer occurs for small enough moments. Rather, increase of radial loading may be continued until substantial deflections are obtained. For the present experiments, it was considered adequate to continue some tests out to deflections of a few wall thicknesses. However, the major attention was given to the determination of critical load combinations for snapping and collapse.

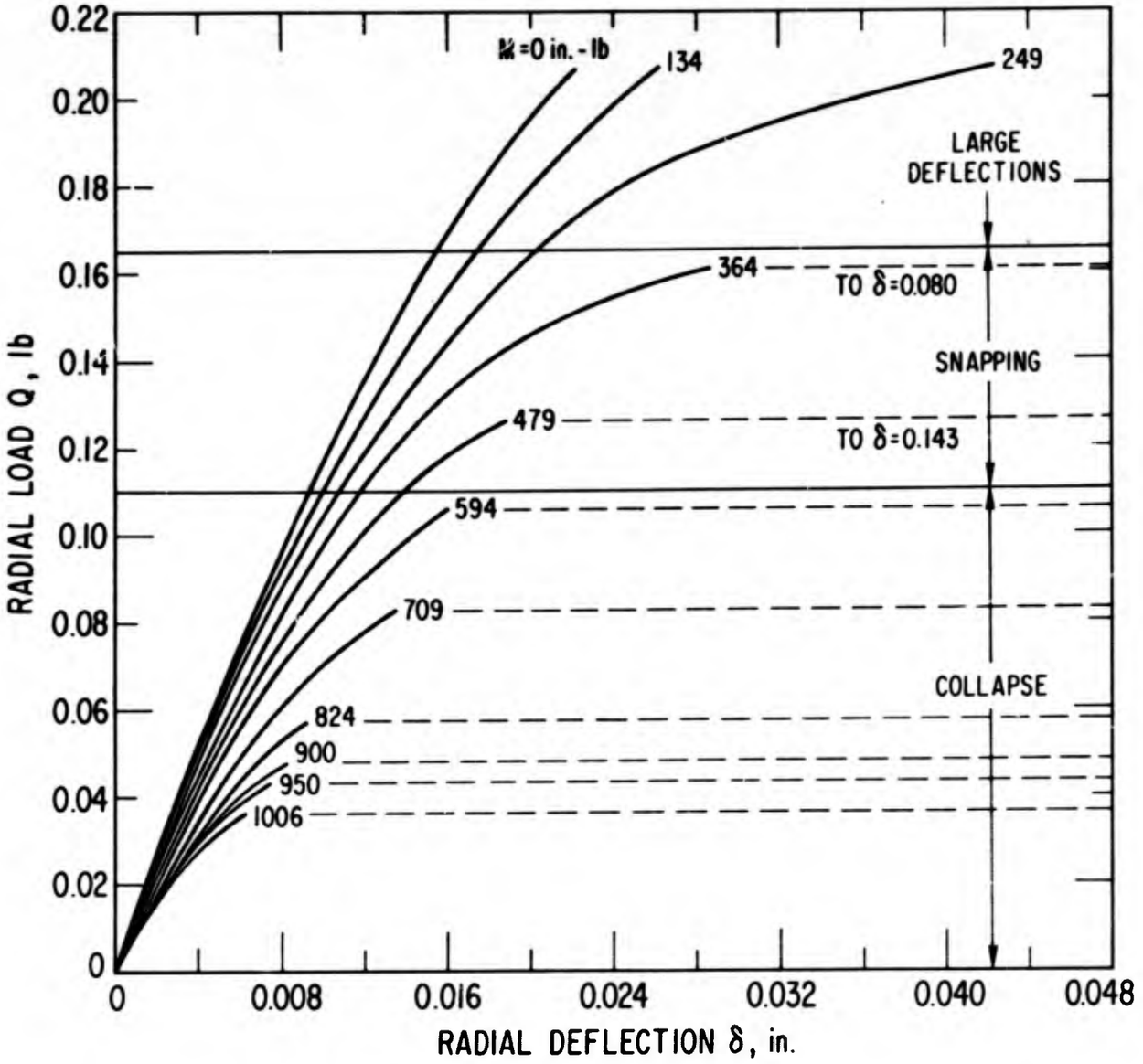

Fig. 5. Radial Load Deflection Characteristics for Shell 4 for Various Bending Moments

Figure 6 gives an interaction plot of typical corresponding critical values of moment M and lateral load Q. Results shown are for Cylinder 4 subjected to spatial distribution of lateral surface loading S_1 and internal pressure p = 0 psi. The heavy solid line denotes a curve fit of test results obtained for a radially inward (compressive) lateral load Q. Also shown are dashed lines, obtained by crossplotting, which indicate the radial center deflection as a fraction of the shell thickness t = 0.014 in. The deflection is measured from the initial undeformed and unstressed state. Observe that repeatability of test results is excellent. It is interesting that there exists a small range of compressive Q's for which the critical buckling moment is not degraded. However, as the compressive lateral loading Q increases, there is a sizeable reduction in the corresponding interaction buckling moment M. Observe that such reductions in M occur when combinations of M and Q are applied which result in net inward (or positive) prebuckling displacements. Tests were also conducted for outward, tensile Q's; but, for the range of parameters investigated, no tensile Q's were found that significantly reduced the critical bending moment.

On the right side of Fig. 6, the critical load curve has two branches: the lower one for snapping, the upper one for collapse. Because of the nearly horizontal slope of the collapse branch, its determination is somewhat sensitive to the order of loading. The discussion to follow pertains to the lower, snapping branch.

Figures 7a (p = 0 psi) and 7b (p = 0.4 psi) show interaction plots of corresponding normalized critical values of moment M and inward lateral loading Q for spatial distribution S_1. Available related interaction data

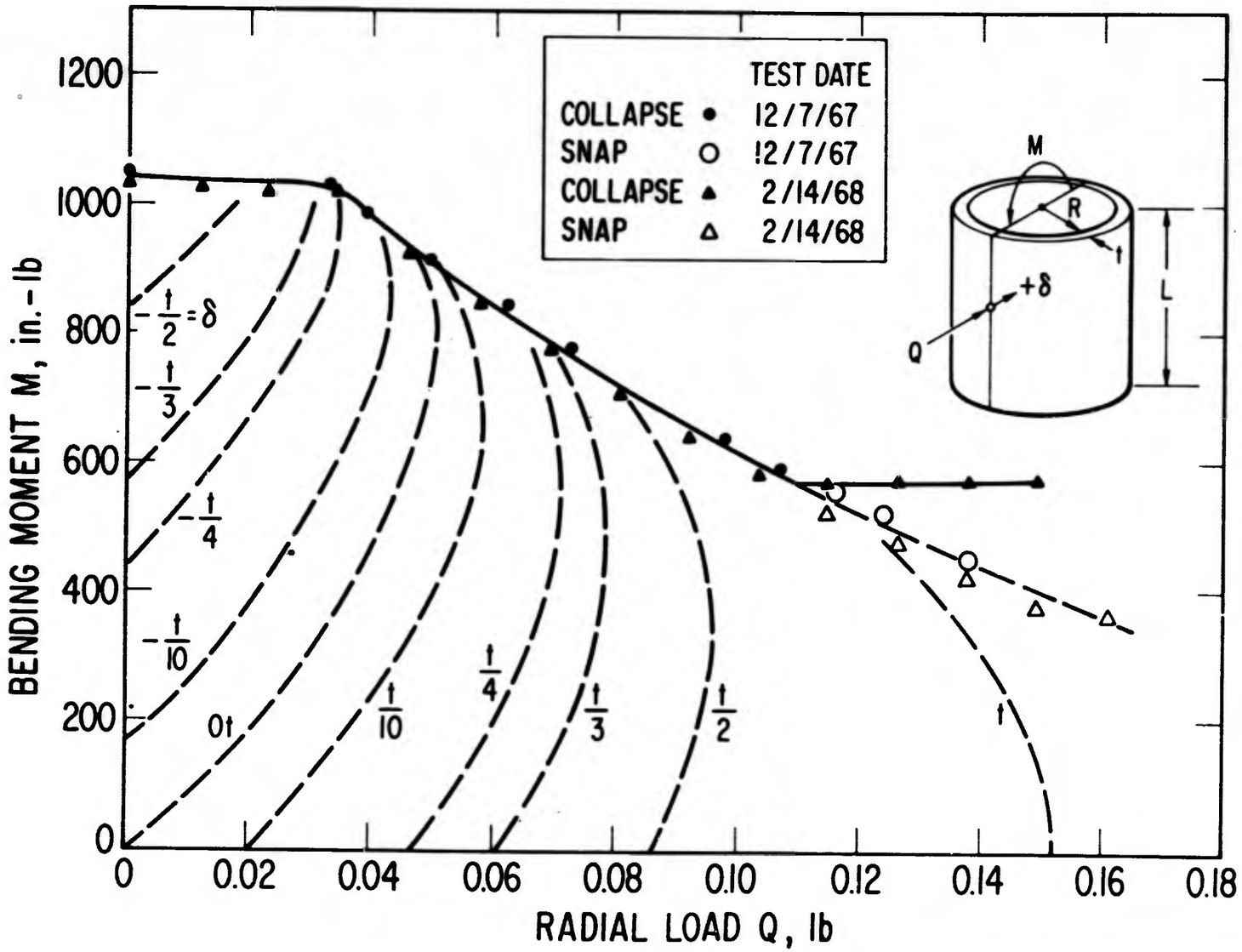

Fig. 6. Critical Load Combinations for Shell 4

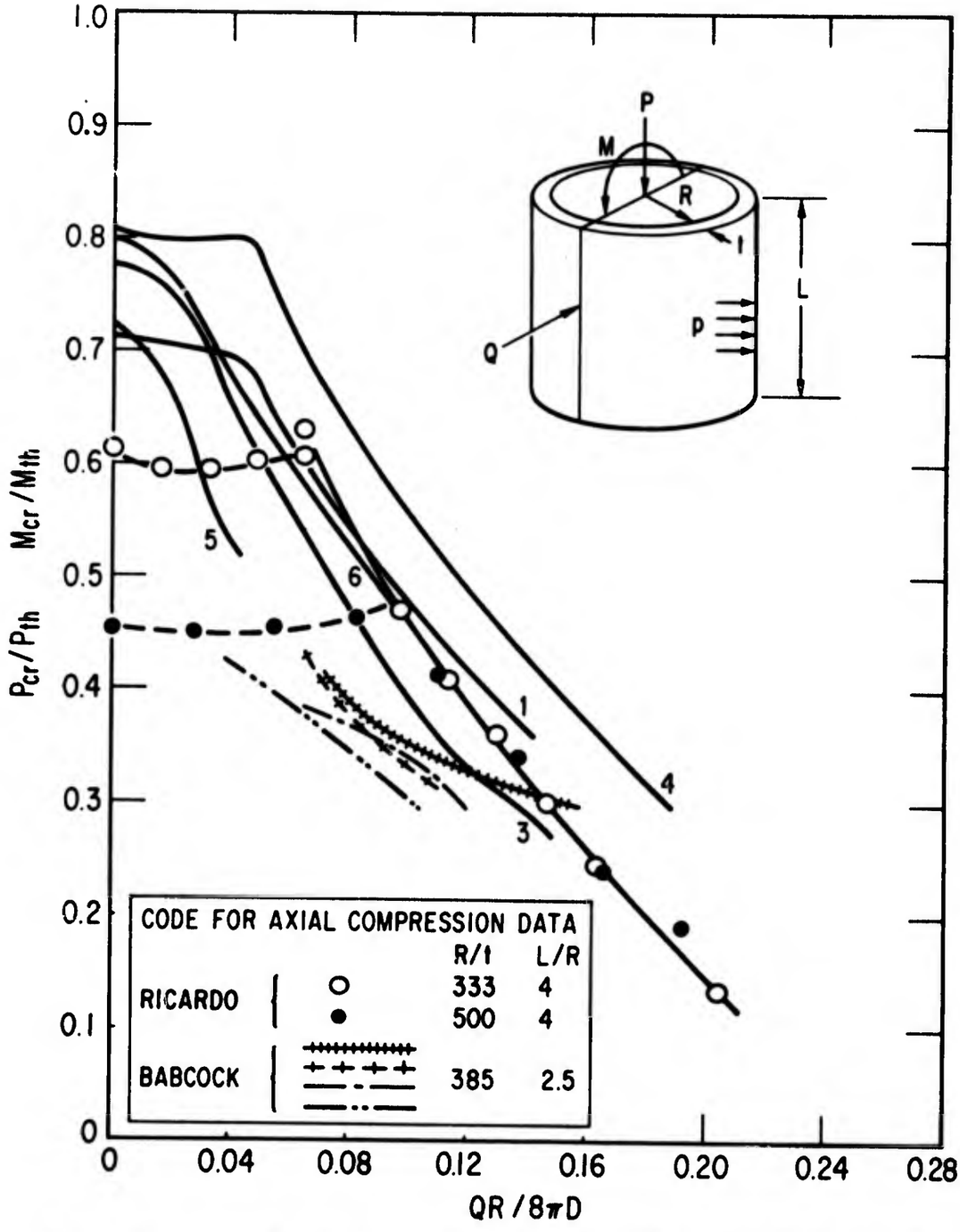

Fig. 7a. Normalized Critical Load Curves for Several Models; Unpressurized, Spatial Distribution S_1

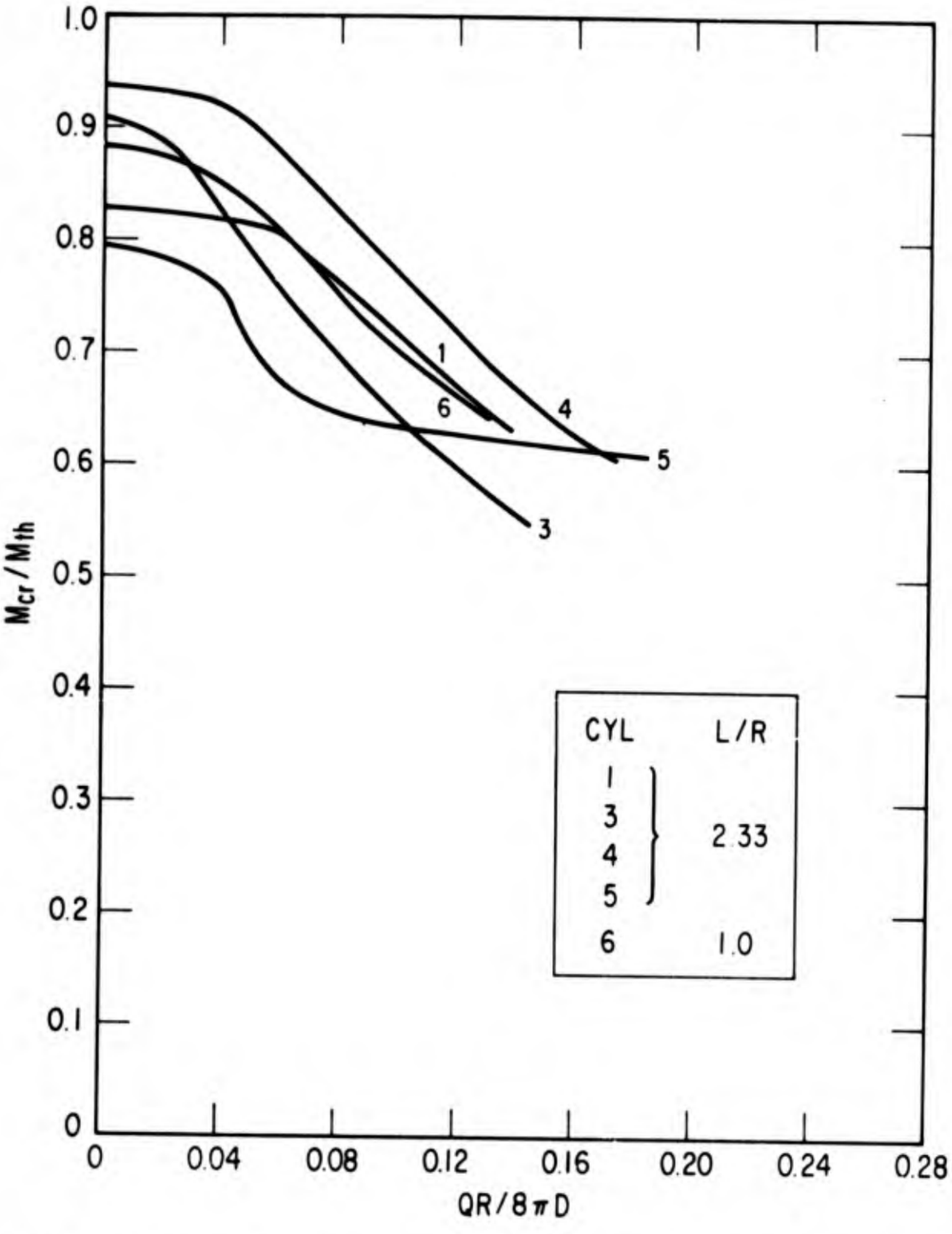

Fig. 7b. Normalized Critical Load Curves for Several Models; Pressurized, Spatial Distribution S_1

for axial compression with p = 0 psi are also shown in Fig. 7a. Here P and Q denote the critical combination of axial and lateral loading. These axial compression data were generated by Ricardo[3] and Babcock[4] from tests on Mylar and brass cylinders respectively. The normalization factors used in Fig. 7 were suggested by Seide[5] and are

$$P_{th} = 2\pi Et^2/[3(1-\nu^2)]^{1/2} \tag{2}$$

$$M_{th} = \pi ERt^2/[3(1-\nu^2)]^{1/2} \tag{3}$$

$$D = Et^3/12(1-\nu^2) \tag{4}$$

Normalization of results as shown here implies greater generality than is perhaps justified from the test data presently available. The reader is cautioned to keep this fact in mind when using these results. For Q = 0, the ratios P/P_{th} and M/M_{th} are in the scatter band of previous test data[2] for cylindrical shells in axial compression and bending. Accordingly, the specimen-to-specimen scatter of test results for finite Q is believed typical of Mylar cylinder laboratory test specimens. Note that the influence of the length-radius ratio is not important for the parameters investigated, but that small internal pressure provides substantial strengthening. From Fig. 7a, it is interesting to observe that axial compression and bending data display the same trend and are in surprisingly good agreement. This follows because either ordinate of Fig. 7 can be interpreted as the ratio σ/σ_{th} where σ is the observed axial buckling stress and

$$\sigma_{th} = (Et/R)[1/3(1-\nu^2)]^{1/2} \tag{5}$$

is the classical theoretical axial buckling stress for $p = Q = 0$.

Figure 8 gives normalized interaction plots of critical values of moment M and inward lateral loading Q for Cylinder 4. Data are presented for spatial distributions of lateral loading S_1 through S_6. Results are shown for both $p = 0$ psi and $p = 0.4$ psi. Again, note the significant increase of interaction buckling allowables brought about by application of only a small internal pressure. The results indicate that the influence of spatial distribution of lateral loading for $p = 0$ psi is of significant importance for the cases considered here, particularly when $QR/8\pi D > 0.04$. Also, observe that the small internal pressure brings the results for all spatial distributions of lateral loading into close agreement. This agreement indicates for the pressure case that there is little or no harmful coupling of prebuckling deformations due to the lateral loads.

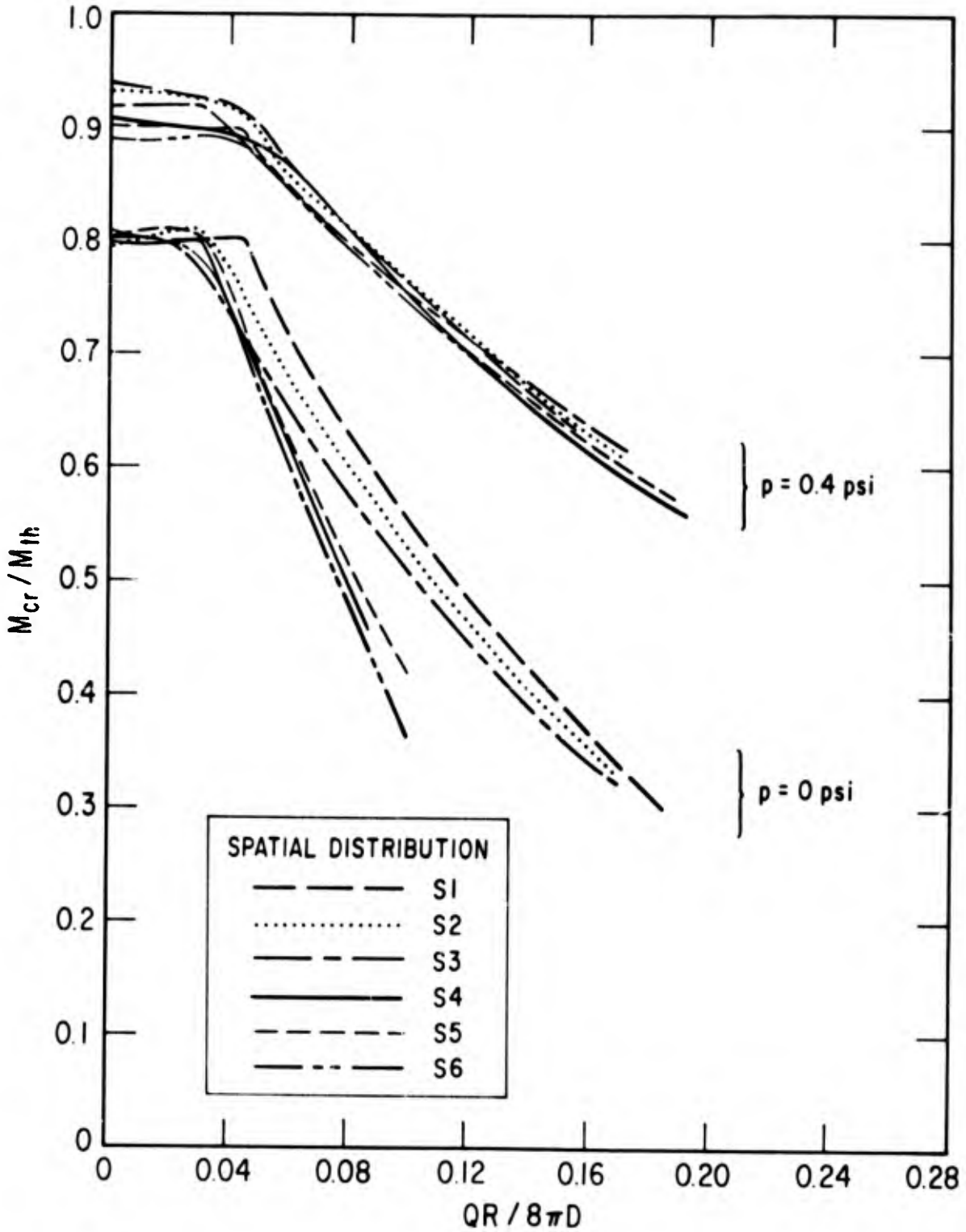

Fig. 8. Effects of Spatial Distributions S_1 Through S_6 on Critical Load Curves for Shell 4

SECTION IV

CONCLUSIONS

It is concluded that concentrated lateral loads can have a considerable degrading effect on the capability of cylinders to withstand a bending moment. Two modes of failure - collapse and snapping - are possible. A small amount of internal pressurization results in a significant strengthening. For the relatively widely spaced spatial patterns considered, multiple radial loads have substantially the same effect as a single radial load. Finally, it appears that a measure of increased generality is obtained for the data by the normalized plot of Fig. 7. This plot shows that all the available data are described by essentially the same curve.

REFERENCES

1. Weingarten, V.I., "Effects of Internal Pressure on the Bending of Circular-Cylindrical Shells Under Bending," Journal of Aeronautical Science, Vol. 29, 1962, p. 804-807.
2. Weingarten, V.I., E.J. Morgan, and P. Seide, Final Report on Development of Design Criteria for Elastic Stability of Thin Shell Structures, STL/TR-60-0000-19425, Space Technology Laboratories, El Segundo, Calif., 1960.
3. Ricardo, O.G., An Experimental Study on the General Buckling of Thin-Walled Circular Cylinders Under Axial Loads, NASA Research Grant No. NsG-18-59, Guggenheim Aeronautical Laboratory, California Institute of Technology, Pasadena, Calif., 1960.
4. Babcock, C., California Institute of Technology, personal communication to P. Wilson concerning tests of brass cylinders performed in 1960, 10 October 1967.
5. Seide, P., Consultant to Aerospace Corporation, personal communication, 28 August 1967.

UNCLASSIFIED

Security Classification

DOCUMENT CONTROL DATA - R&D

(Security classification of title, body of abstract and indexing annotation must be entered when the overall report is classified)

1 ORIGINATING ACTIVITY *(Corporate author)*
Aerospace Corporation

2a REPORT SECURITY CLASSIFICATION
Unclassified

2b GROUP

3 REPORT TITLE
INFLUENCE OF CONCENTRATED LATERAL LOADS ON THE ELASTIC STABILITY OF CYLINDERS IN BENDING

4 DESCRIPTIVE NOTES *(Type of report and inclusive dates)*

5 AUTHOR(S) *(Last name, first name, initial)*
S. Okubo, J.S. Whittier, P.E. Wilson

6 REPORT DATE
68 DEC 15

7a TOTAL NO. OF PAGES
27

7b NO OF REFS
5

8a CONTRACT OR GRANT NO
F04701-68-C-0200

b. PROJECT NO

c

d

9a ORIGINATOR'S REPORT NUMBER(S)
TR-0200(9990)-1

9b OTHER REPORT NO(S) *(Any other numbers that may be assigned this report)*
SAMSO-TR-69-55

10 AVAILABILITY/LIMITATION NOTICES
~~Qualified requesters may obtain copies of this report from DDC.~~
This document has been approved for public release and sale; its distribution is unlimited.

11 SUPPLEMENTARY NOTES

12 SPONSORING MILITARY ACTIVITY
Space and Missile Systems Organization
Air Force Systems Command
Los Angeles Air Force Station
Los Angeles, California

13 ABSTRACT

The character of the instability and the degradation of the moment-carrying capacity are found by Mylar model experiments for cylinders in bending when subjected to concentrated lateral loads. Lateral loads can seriously degrade the moment capability of cylinders. Critical combinations of moment and lateral load cause two distinct modes of failure - collapse and snapping. Collapse modes exhibit buckles which cover the compression half of the cylinder and are critical for large values of moment and small values of lateral load. Snapping modes of failure involve a single dimple and exist for smaller values of moment and larger values of lateral load.

DD FORM (FACSIMILE) 1473

UNCLASSIFIED

Security Classification

14

KEY WORDS

Cylindrical Shells
Test Results
Concentrated Loads
Elastic Stability
Bending Moment
Mylar Cylinder

Abstract (Continued)